1990 25TH Intersociety Energy Conversion Engineering Conference

Vol. 4

IECEC-90
August 12-17, 1990
Reno, Nevada

Participating
Societies

PROCEEDINGS OF THE 25th INTERSOCIETY ENERGY CONVERSION ENGINEERING CONFERENCE

VOLUME 4

Energy Systems
- Thermal Management
- Conservation
- Transportation
- Environmental Issues
- Mechanical and Thermal Storage
- Alternative Fuels

Policy Impact on Energy
- Energy for Developing Countries
- Greenhouse Effect on Energy Choices
- Domestic Policies

Editors:
Paul A. Nelson
William W. Schertz
Russell H. Till

AMERICAN INSTITUTE OF CHEMICAL ENGINEERS

345 East 47th Street • New York, New York 10017

PROCEEDINGS OF THE 25th INTERSOCIETY ENERGY CONVERSION ENGINEERING CONFERENCE

ISBN 0–8169–0490–1

CONTENTS

NOTE: Please check Post-deadline Section in Volume 6 for any missing papers.

ENERGY SYSTEMS AND POLICY IMPACT ON ENERGY

THERMAL MANAGEMENT—SESSION 27.1

CONSERVATION I—SESSION 28.1

THERMAL ENERGY STORAGE SYSTEMS FOR HEATING AND COOLING SESSION 31.3

THERMAL ENERGY STORAGE—ICE TECHNOLOGY—SESSION 31.4

NOVEL COOL AND CHILL STORAGE SYSTEMS—SESSION 31.5

A Laminar-Flow Heat Exchanger

F. D. Doty, G. Hosford, J. D. Jones & J.B. Spitzmesser

Doty Scientific Incorporated & Simon Fraser University

Abstract

The advantages of designing heat exchangers in the laminar flow regime are discussed from a theoretical standpoint. It is argued that laminar flow designs have the advantages of reducing thermodynamic and hydrodynamic irreversibilities, and hence increasing system efficiency. More concretely, laminar flow heat exchangers are free from the turbulence-induced vibration common in conventional heat exchangers, and can thus offer longer life and greater reliability.

The problems of manufacturing heat exchangers suited to laminar flow are discussed. A method of manufacture is outlined which allows compact, modular design. Experience with this method of manufacture is described, and experimental results are presented.

The problems of fouling and flow maldistribution are briefly discussed, and some possible applications mentioned.

Introduction

Heat exchanger design always involves a compromise between three objectives: maximizing the heat exchanger effectiveness; minimizing the work required to overcome fluid friction in the heat exchanger; and minimizing the manufacturing and material costs of the exchanger. In the past, the third objective has pushed design in the direction of high-turbulence heat exchangers, to take advantage of the high heat transfer coefficient associated with turbulent flow. But with respect to the first two objectives this is a poor choice: turbulent flow exacts a disproportionately high penalty in pumping work, and the vibration engendered by turbulence shortens the life of the equipment. Second-law analysis shows us that high efficiency heat exchangers must be non-turbulent with minimum temperature difference between counterflowing streams [1].

By taking advantage of modern manufacturing techniques, we can produce heat exchanger designs that would have been impossible at the time that current design practices evolved. This allows us to seek greater reliability and higher efficiency by exploring designs that operate in the laminar flow regime. In the following paragraphs, we establish some of the basic design principles that hold in that regime. Our first interest is in gas-to-gas heat exchangers, though some of our remarks will also apply to liquid-gas and liquid-liquid heat exchange.

It will be shown below that it is desirable to operate at very high static pressures (1 to 5 MPa) to minimize the flow velocity. Mechanical stress considerations therefore favor a tubular design.

Current practice in compact heat exchangers is dominated by crossflow designs because they are thought to simplify manifolding problems. However, crossflow has a maximum practical effectiveness of 50% for symmetric flow conditions and pumping power losses are increased due to unavoidable turbulence. Several crossflow exchangers may be used in series to achieve higher effectiveness, but a counterflow exchanger is the only practical method of approaching 100% effectiveness under symmetric flow.

A counterflow heat exchanger module is shown in Fig. 1. It consists of a large number of small tubes, manifolded together in parallel, with a surrounding cage to establish counterflow conditions. Counterflow exchangers have been used for decades to achieve very high heat recovery [2]. In theory it has never been difficult to achieve 95% effectiveness, but in practice this has required prohibitively large and expensive exchangers for gases. We find that a 95% effective heat exchanger currently costs at least 8 times as much as a 60% effective design.

For large-scale production of heat exchangers, as for most other goods produced on a sufficiently large scale, the dominant cost is that of the raw materials used [3]. This is especially true when novel manufacturing techniques reduce manufacturing costs by several orders of magnitude. For this reason, power density or specific conductance (W/kgK) is one of the most significant figures of merit for a heat exchanger. We show below how this figure can be maximized for a laminar counter-flow heat exchanger, while keeping the pressure drop and axial conduction losses within reasonable bounds. We then test this analysis against experiment. In summary, our analysis shows that we should reduce tube diameter to the smallest value it is feasible to manufacture, keeping pressure drop in check by shortening the tubes, increasing their number and perhaps increasing the operating pressure.

Theoretical Analysis of Laminar-Flow Heat Exchangers

Heat exchangers are generally evaluated in terms of their *effectiveness*, E, where effectiveness is defined as the ratio of heat actually transferred to that which would be transferred by a heat exchanger having infinite heat transfer area and operating under the same conditions. It may be shown that for a counter-flow heat exchanger exchanging heat between two fluid streams, mass flow rates $\dot{m}_C$ and $\dot{m}_H$, specific heats c_C and c_H, the effectiveness is given by [4]:

$$E = \frac{1 - e^{-NTU(1-R)}}{1 - Re^{-NTU(1-R)}} \tag{1}$$

where NTU denotes the number of transfer units:

$$NTU = \frac{UA}{c\dot{m}} \tag{2}$$

c and $\dot{m}$ being the specific heat and mass flow rate of the fluid stream having the lesser heat capacity, and where R denotes the ratio of the lesser heat capacity to the greater:

$$R = \frac{c_{\min}\dot{m}_{\min}}{c_{\max}\dot{m}_{\max}} \tag{3}$$

If the capacities of the two streams are equal, the right-hand side of Eq. 1 becomes undefined and must be replaced by the simpler expression

$$E = \frac{NTU}{NTU + 1} \tag{4}$$

For laminar flow conditions, it is well known that the heat exchange capacity of a tube is independent of tube diameter and gas velocity (See, for example, Problem 14c on p. 108 of [5].) The independence of Nusselt number, Nu, from Reynolds number, Re, for laminar flow indicates that heat transfer between tube-side and shell-side is determined solely by the two fluid conductivities and geometric factors.

Consider a tubular counterflow heat exchanger made up of n tubes, length L, internal diameter d_i, with laminar flow within and without. We shall assume that the fluid flowing within the tubes is the hotter on entry. We may take the conductivity of the tube material to be large compared with that of the two fluids, and hence write:

$$UA = 4\pi nL\left(\frac{k_C k_H}{ak_C + bk_H}\right) \tag{5}$$

where k_H and k_C are the thermal conductivities of the inner and outer gases respectively, and a and b are dimensionless coefficients of the order of unity that are functions of tube inner and outer diameters and tube spacing. (It is acknowledged that this treatment is unconventional; we claim, however, that it correctly represents the relevant physical dependencies, and that it may reasonably be used to establish a qualitative design strategy.) For tube centers spaced $2d_i$, with tube wall $w = 0.2d_i$, a is approximately 0.7 and b is unity. We will assume these geometric relationships and take $k_C = k_H$ for the remainder of this discussion.

In addition to achieving a certain effectiveness, the designer will be concerned with the cost of the heat exchanger, the pumping losses, and conduction losses. We shall also insist that the flow remains laminar. Constraints can be written down corresponding to these requirements. In the following paragraphs, we shall develop the constraints for the tube-side flow; the arguments for shell-side flow are very similar.

In conventional heat exchanger design, machining and assembly costs overshadow the cost of the materials used. However, for reasons to be explained below, we shall consider material costs as primary. The mass of material required for the microtubes in a heat exchanger is then

$$M = 0.24\pi d_i^2 nL\rho_m \tag{6}$$

The tube-side pumping power loss $\dot{W}_p$ can be expressed in terms of the tube-side mass flow rate $\dot{m}_H$ as follows [6]:

$$\Delta p = \frac{128\mu L\dot{m}_H}{\rho n\pi d_i^4}$$

$$\Rightarrow \dot{W}_p = \frac{128\mu L}{n\pi d_i^4}\left(\frac{\dot{m}_H}{\rho}\right)^2 \tag{7}$$

where ρ is the gas density (kg/m³) and μ is the dynamic viscosity (kg/ms). We shall write this as

$$\dot{W}_p = \frac{128\mu\dot{m}_H^2}{\rho^2\pi}\Omega \tag{8}$$

where Ω denotes the group L/nd_i^4.

We are going to propose a design made up of many short narrow tubes. As we move towards such a design, a loss mechanism not previously important becomes significant — longitudinal thermal conduction through the tube metal from the hot end to the cool end. We denote the heat flow via this pathway by $\dot{W}_m$. Accurate calculation of this effect is difficult; a good treatment is provided by [7], pp. 4-53–4-56. For typical microtube heat exchanger designs, $\dot{W}_m$ is about 0.3% of the heat exchange power, so we introduce no serious inaccuracy by treating conduction losses through the tube material as decoupled from the flowing fluid.

$$\dot{W}_m \approx \frac{0.2n\pi d_i^2 k_m(T_H - T_C)}{L} = \frac{0.2\pi k_m(T_H - T_C)}{\Omega d^2} \tag{9}$$

where k_m is the tube metal conductivity, and T_H and T_C are the hot and cold temperatures respectively. It is predominantly this loss mechanism which establishes the theoretical limit to specific conductance (minimum tube diameter) in high-efficiency counterflow exchangers.

Lastly, the condition that the internal flow be laminar is expressed by

$$Re = \frac{4\dot{m}_H}{n\pi d_i\mu} \leq 2300 \tag{10}$$

Let us suppose that there is some combination of the parameters n, L and d_i that gives a satisfactory value for effectiveness and gives acceptable levels of flow losses and conduction losses. We argue that, whatever the initial values are, it will always be possible to apply the following strategy: reduce d_i by a factor p; simultaneously increase n and decrease L, each by a factor p^2, thus keeping flow losses and UA, hence E, constant. This change will maintain laminar flow while reducing system mass by a factor p^2. We can reduce d_i until either conduction losses become unacceptable or until we go below the limits of manufacturability. The motivation for reducing d_i in this way is provided by Equation 6: mass, and hence, given our assumptions, cost, goes down as p^2.

It is straightforward to calculate a value of d_i typical of this design method. Let us suppose that for a given application, the pumping power may not exceed 1% of the ideal heat exchange power. Then

$$\frac{\dot{W}_p}{\dot{m}c(T_H - T_C)} \leq 0.01 \tag{11}$$

Substituting from Eq. 8 and rearranging:

$$\Omega \dot{m} \leq \frac{\pi c(T_H - T_C)\rho^2}{12800\mu} \tag{12}$$

Taking the maximum permitted value of $\Omega \dot{m}$ from Eq. 12, we consider the limit imposed by conduction losses. Let us also require that conduction losses not exceed 1% of the ideal heat exchange power. Then

$$\frac{\dot{W}_m}{\dot{m}c(T_H - T_C)} \leq 0.01 \tag{13}$$

Substituting from Eq. 9 and rearranging, then substituting from Eq. 12 gives:

$$\Omega d_i^2 \dot{m} \geq \frac{20\pi k_m}{c}$$
$$\Rightarrow d_i^2 \geq \frac{20\pi k_m}{c\dot{m}\Omega}$$
$$\Rightarrow d_i \geq \sqrt{\frac{20 \times 12800\mu k_m}{\rho^2 c^2 (T_H - T_C)}} \tag{14}$$

Evaluating Eq. 14 for a stainless-steel heat exchanger with helium at 1 MPa as the working fluid, operating between temperatures of 900 and 300 K, we obtain a lower limit on tube diameter of about 90 microns. This figure is typical of the dimensions yielded by this design method, and is about an order of magnitude smaller than appears feasible from manufacturing and corrosion considerations. This establishes that, given our assumptions, it is desirable to design for the finest-diameter tubes feasible. (We have only examined tube-side flow, but a similar argument would lead to the same conclusions for shell-side flow.)

It may be questioned, however, whether our assumptions are reasonable. For some space applications, reducing heat exchanger mass is desirable in itself. To show that our technology is practical for terrestial applications, we must show that we can so reduce the cost of machining and assembly that material costs come to predominate; we must also address the problem of fouling and flow maldistribution. Before dealing with these questions, we will fill out the above calculation with a complete design example, then describe an experimental test of the theory.

Let us suppose that the helium in the above example is flowing at 1 kg/s, and that we wish to exchange heat between this and another gas stream, flowing at the same rate, with an effectiveness of 95%. Substituting the appropriate values of physical constants in Eq. 2, 4 and 5 and rearranging, we obtain:

$$nL \geq 94000\text{m} \tag{15}$$

We shall continue to require that the pumping power needed to overcome fluid friction be less than 1% of the heat exchange power. Using Eq. 7, we obtain

$$\frac{n}{L} \geq 100 \frac{128\mu}{\pi c(T_H - T_C)d_i^4}\left(\frac{\dot{m}}{\rho}\right)^2 \tag{16}$$

In accordance with our design strategy, we select the smallest value for d_i that it is practical to manufacture. We shall show below that this value is about 0.5 mm. Substituting for d_i and the other parameters, we obtain

$$\frac{n}{L} \geq 900000 \tag{17}$$

Combining Eq. 15 and 17 gives $L \approx 0.3$ m and $n \approx 300000$. For very large-scale applications, the number of parallel tubes will be numbered in the millions, requiring thousands of parallel modules to maintain uniform shell-side flow. Such geometries are unusual for counterflow heat exchangers, but are quite typical of regenerative heat exchangers such as gas turbine rotating-porous-ceramic-wheel recuperators or Stirling cycle wire-mesh regenerators.

Method of Manufacture

The discussion above assumes that manufacturing cost can be treated as primarily dependent on heat exchanger mass. As every heat exchanger designer knows, this is not currently the case. If our discussion of design is to be of more than academic interest, we must therefore show that a practical method of manufacture can be found.

To realise the unconventional heat exchanger designs required by the above theory, we manifold together large numbers of identical modules, each module containing several hundred tubes. Each module is about 100 mm long; this length represents a compromise between the need to minimize conduction losses and the tendency of longer tubes to distort during the manufacturing process. The modules can be manifolded in series to achieve multiples of this length. A typical module is shown in Fig. 1.

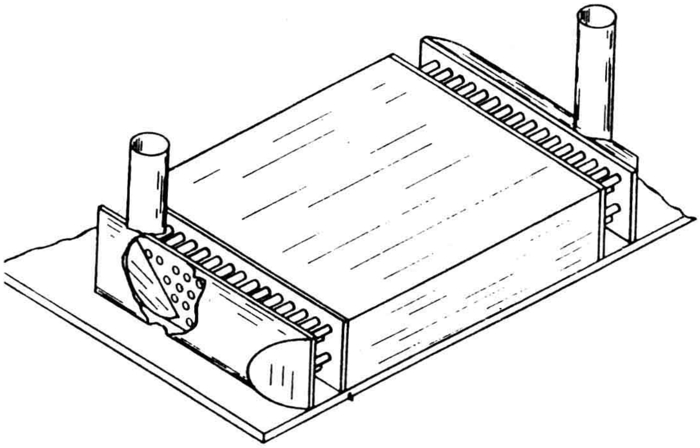

Figure 1

To facilitate uniform shell-side flow and to permit fineblanking of the header tubestrips, it is necessary to depart from the disc-shaped header tubesheet normally used in heat exchangers and use a rectangular header tubestrip, as shown, with fewer than ten rows of tubes.

Advances in high-speed laser welding technology and diamond dies make it possible to produce very small stainless steel tubing at low production costs — less than \$0.14 per meter [8]. These can be joined to the endplates by diffusion welding:

Advances in Diffusion Welding Technology

Diffusion welding occurs when clean metal surfaces are held together under pressure at high temperatures. The combined action of solid-state diffusion mechanisms and solid-state surface tension result in recrystallization or grain growth across an interface and the solution or dispersion of interfacial contaminants [9]. The time required to form the bond is an inverse exponential function of temperature and a quadratic function of surface finish and interfacial gaps. For most nickel-chromium alloys with precision surfaces (0.4 μm rms) under moderate pressure (5 MPa, or 700 psi), high-quality welds (90% of the base metal strength) can be obtained in several seconds at 1230°C.

Method of Assembling Tube Arrays

We have developed a technique for joining microtubes to header strips *en masse.* The technique permits tube alignment, insertion, and welding rates to exceed 1,500,000 pieces per day per production line at an estimated production cost of less than $0.01/tube.

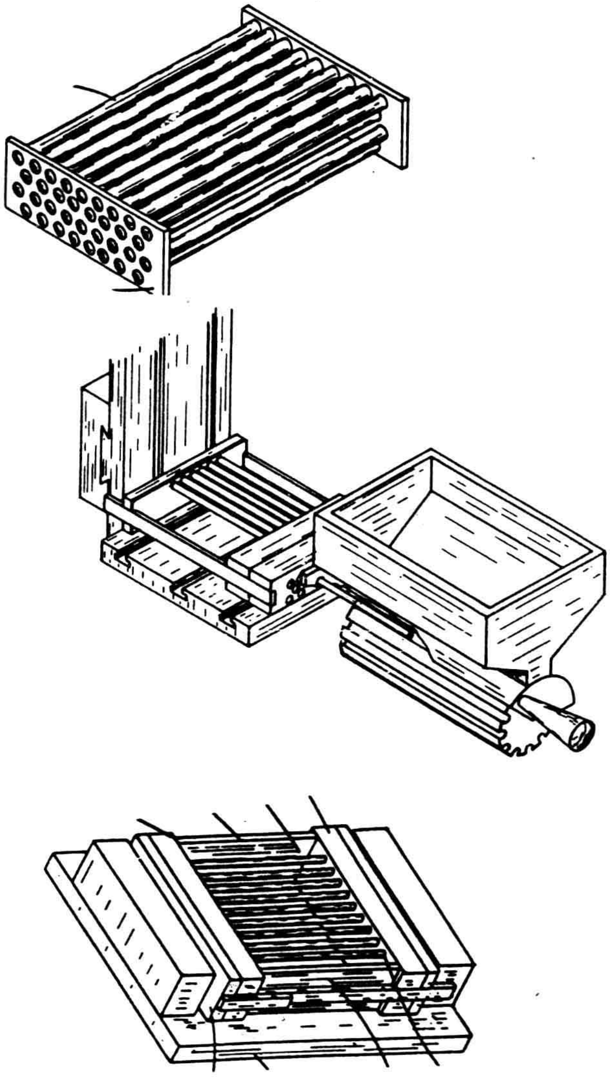

Figure 2a,b,c

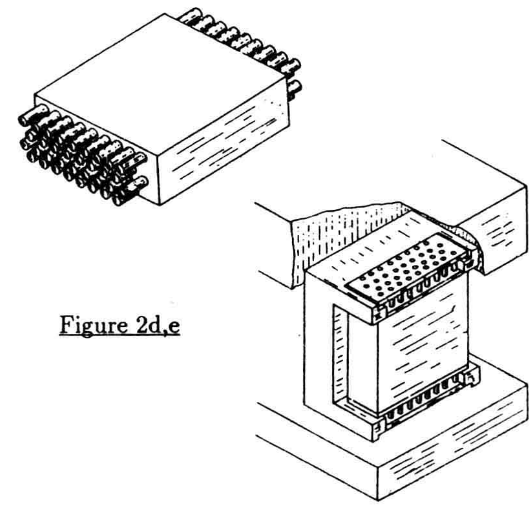

Figure 2d,e

The following sequence of operations is followed: the tubes are finished to the required length; the tubes are inserted into adjacent, parallel, precision, non-sacrificial spacer forms, similar in size and pattern to the header tubestrips but with precision, slip-fit, countersunk holes (Fig. 2a), using a hopper-and-Gatling-gun arrangement (Fig. 2b). Next, the spacer forms are slid apart to near opposite ends of the tubes; caps are placed over the ends of the tubes to secure the tube ends (Fig 2c) and the tube-spacer-cap fixture assembly is placed in a mold suitable for vacuum injection. The mold is evacuated and a molten, fusible alloy is injected into the heated mold. The mold is then cooled below the solidus temperature, the encapsulated assembly removed and the securing caps and spacer forms slid off, exposing the tube ends (Fig. 2d). Lastly, the assembly is loaded into a suitable fixture on a press and the header tubestrips pressed onto opposite ends of the tubes (Fig. 2e; the typical force required for 1000 1-mm tubes is 10^5 N, about 10 tons). The fusible alloy is melted and cleaned from the assembly by a combination of melting, vibration, and air jets, followed by chemical cleaning.

Suitable weld conditions are readily achieved if the tube diameter and hole size can be held to very tight tolerances. The use of hardened tubes and annealed tubestrips then makes it possible to press the tubes into slightly undersized holes in the thin, rectangular, header tubestrip. With hard, straight tubes, of length less than 300 times their O.D., it is possible to press them into soft tubestrips with up to 3% interference without serious difficulty. With proper attention to surface quality and a minimum of 0.4% interference fit, the conditions required for diffusion welds are readily achieved. Surface finishes of about 0.4 μm rms in the area of the diffusion weld have proven to be 100% leak-tight — within 10^{-6} standard mm^3/s to hydrogen at one atmosphere.

After the header tubestrips have been pressed onto the microtubes and the assembly of microtubes and header tubestrips is thoroughly cleaned, it must be heated to effect the diffusion weld to the tubes. Most of our diffusion welding thus far has been done in inert or reducing atmosphere ovens and consequently has been limited to slow cycles. Numerous experiments are required to determine optimum surface preparation techniques, atmosphere, interference, and temperature cycle for diffusion welding. About ten seconds at 1230°C appears sufficient for full-strength diffusion welds in the Ni-Cr-W superalloy Haynes 230.

Advances in Fineblanking Technology

The requirement of low production costs in the hard-drawn 1-mm tubing imposes a tolerance limit of ±0.4%, which then leaves a ±0.9% tolerance requirement for the hole diameters in the tube-strip. Fortunately, the hole diameter need not be constant over the majority of its length, and a slight taper is in fact beneficial in assembly. Punching consistently suitable, closely spaced microholes in superalloys does represent a major technical challenge. Our initial prototypes used drilled holes, followed by reaming. More recently, we have successfully used tubestrips produced by Swiss fineblanking – a controlled cold-flow blanking (punching) process that includes the use of a counter-punch and a high pressure ring indenter (stripper) which applies sufficient pressure to the metal surfaces near the punch edges to prevent normal and planar deformation of the material during punching [11]. The technique requires compound dies and triple-action presses, but results in minimal edge fracturing and deformation.

No other technique can come close to competing on a cost basis in large scale production with Swiss fineblanking — less than $1 per tubestrip. However, electrochemical and electrical discharge techniques are likely to permit even smaller holes with closer spacing. We also plan to evaluate these techniques — especially for small scale, ultra-high density applications.

Experimental Results

We have assembled several dozen fully welded prototype 103-tube MTS modules similar to the one shown in Figure 1. The modules used 0.33 mm ID tubes, 127 mm in length, with 0.1524-mm walls. The tube-strip has 5 rows of tubes with 21 holes in the odd-numbered rows and 20 holes in the even-numbered rows, arranged in a triangular pitch on 1.25-mm centers. Three modules were assembled into shells with manifolds to distribute tube-side and shell-side flows, and baffles between the modules to promote uniform shell-side flow through each module.

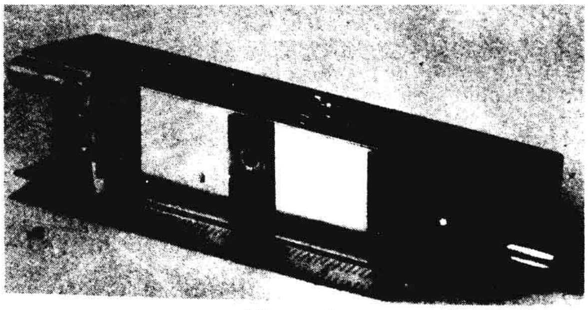

Figure 3

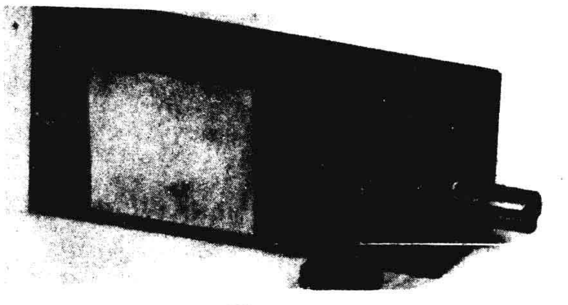

Figure 4

Figure 3 shows the modules, baffles, manifolds and partially assembled shell. Figure 4 shows a finished prototype bank. The entire assembly has an overall length of 190 mm, a height of 30 mm, a width of 35 mm and a total mass of 0.3 kg. Scaling up to a bank with greater numbers of modules and more tubes per module would reduce the specific mass of the bank by up to 70%.

The finished bank was used for gas-gas heat exchange, using the experimental set-up diagrammed in Figure 5.

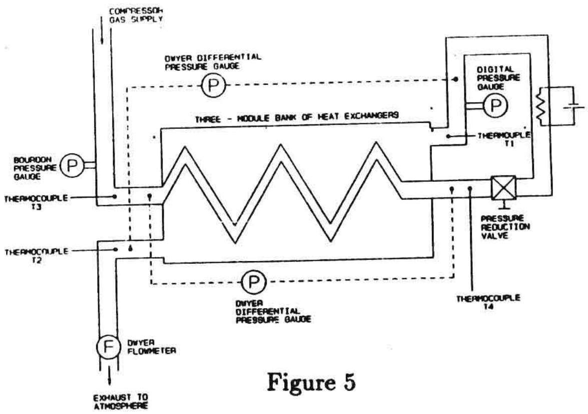

Figure 5

High-pressure gas from a bottled supply was supplied to the tube-side, its inlet and outlet temperatures, T_3 and T_4, being measured using sheathed and grounded 1.6-mm Type 4 chromel-alumel thermocouples. The outlet gas was then expanded through a pressure-reduction valve, electrically heated, and allowed to flow through the shell-side, inlet and outlet temperatures T_1 and T_2 again being measured with unshielded chromel-alumel thermocouples. The outlet gas was exhausted to atmospheric pressure, its volumetric flow rate being measured with a Dwyer floating-ball flowmeter. Pressure drops across tube-side and shell-side were measured using Dwyer differential pressure transducers. Following each change in gas flow rate, care was taken to ensure that flowmeter and thermocouple readings reached steady values before any measurements were taken.

Data Reduction

To compare the experimental results with our theoretical analysis, we calculate the effectiveness of the heat exchanger from the temperature measurements T_1, T_3 and T_4. Since the thermal capacities of the hot and cold streams are equal, we can invert Equation 4 to calculate NTU from effectiveness:

$$NTU = \frac{E}{1-E} \tag{18}$$

We calculate UA from

$$UA = \frac{\dot{m}c_p\Delta T}{T_\delta} \tag{19}$$

where ΔT is the temperature drop between T_1 and T_2 and T_δ is the mean temperature difference between hot and cold streams. We compare this with the value predicted by our Equation 5, using tabulated values for k_C and k_H, evaluated at the mean tube-side and shell-side temperatures respectively. Similarly, we compare measured values of Δp with those calculated from Equation 7. The errors for each calculated quantity are estimated using Theorem 3 from [12].

$\dot{m}$ (mg/s)	p (kPa)	T_1 (C)	T_2 (C)	T_3 (C)	T_4 (C)	E(%)	NTU	UA(W/K)	UA(Eq. 5)
Nitrogen									
470± 20	322±3	104.7±0.5	30.9±0.5	23.0±0.5	93.0±0.5	85.7±0.6	6.0±0.3	3.7±0.4	7.1
840± 20	322±3	96.5±0.5	32.3±0.5	23.3±0.5	84.1±0.5	83.1±0.7	4.9±0.2	5.3±0.5	7.1
930± 20	322±3	99.4±0.5	33.0±0.5	22.8±0.5	85.8±0.5	82.2±0.7	4.6±0.2	5.4±0.5	7.1
373± 20	705±3	51.4±0.5	28.5±0.5	26.1±0.5	48.8±0.5	89.7±0.7	8.7±0.6	3.5±1.4	7.1
738± 20	1462±3	64.7±0.5	28.9±0.5	25.3±0.5	59.2±0.5	86.0±0.7	6.1±0.4	6.0±1.3	7.1
1085± 20	1068±3	64.8±0.5	28.6±0.5	23.6±0.5	58.3±0.5	84.2±0.7	5.3±0.3	7.1±1.2	7.1
1413± 20	1486±3	67.3±0.5	29.3±0.5	22.9±0.5	59.5±0.5	82.4±0.7	4.7±0.2	7.9±1.1	7.1
1824± 20	1470±3	58.1±0.5	23.3±0.5	15.3±0.5	48.8±0.5	78.2±0.7	3.6±0.1	7.6±0.9	7.1
Helium									
117±7	749±3	107.5±0.5	28.3±0.5	23.5±0.5	103.6±0.5	95.4±0.6	21±3	11.1±2.5	39.0
79±7	756±3	103.8±0.5	29.5±0.5	24.0±0.5	100.5±0.5	95.7±0.7	22±4	6.9± 1.6	39.0
213±7	825±3	109.4±0.5	28.7±0.5	23.1±0.5	103.4±0.5	93.0±0.7	13.3±1.4	15.4±2.6	39.0

Table 1

The most serious source of error arises from the small values of T_δ at high effectiveness; this may be remedied by the use of differential thermocouples.

The values of UA calculated from Equation 5 are obtained setting the dimensionless parameters a and b to unity. These calculated values agree quite well with the experimental results for moderate values of effectiveness (75-85%). At higher values of E, however, there is clearly a discrepancy between theory and experiment, which we believe to result from flow maldistribution. In support of this belief, we note that the discrepancy is most serious at low flow rates, consistent with the findings of Mueller and Chiou [13].

The increase in UA with flow rate might be attributed to turbulence, but we think this unlikely: the maximum tube-side Reynolds number was approximately 1400 for nitrogen, 160 for helium. Turbulence would also be expected to result in measured values of Δp higher than predicted by Equation 7.

$\dot{m}$ (mg/s)	p (KPa)	Δp (kPa)	Δp (Eq. 7)
Nitrogen			
470± 20	322±3	5.1±0.2	3.7±0.2
840± 20	322±3	9.5±0.2	6.6±0.2
930± 20	322±3	11.1±0.2	7.3±0.2
373± 20	705±3	1.3±0.05	1.3±0.2
738± 20	1462±3	1.5±0.05	1.3±0.2
1085± 20	1068±3	3.3±0.1	2.5±0.2
1413± 20	1486±3	3.7±0.1	2.3±0.2
1824± 20	1470±3	5.5±0.2	3.1±0.2
Helium			
117±7	749±3	2.3±0.1	3.0±0.2
79±7	756±3	1.5±0.05	2.0±0.2
213±7	825±3	4.4±0.1	5.5±0.2

Table 2

Tube-side pressure drops were also measured, and are reported in Table 2. These results are reasonably well predicted, though experimental results for helium are somewhat lower than expected. This is consistent with minor tube-side maldistribution, though we expect the major maldistribution problems to be on the shell side.

Even given the extent to which measured heat transfer falls short of theoretical performance at high E, the absolute values of specific conductance demonstrated are quite encouraging, with a figure of 50 W/K.kg for the sixth test.

Operational Problems

We have argued that a laminar-flow design is theoretically appealing, and reported some experience with the manufacture of a prototype. Several major questions, however, must be addressed before heat exchangers of the MTS type can be considered for practical use.

Fouling

Fouling is often a serious problem for heat-exchanger designs characterised by very narrow flow passages, as is the MTS heat exchanger. Marner and Suitor point out in their review of this area that fouling exacts a double penalty, reducing effectiveness and increasing pressure drop [14]. In the laminar-flow regime, if the fouling is uniform between tubes and the conductivity of the deposit is high compared with that of the working fluid, Equation 5 suggests that the effectiveness penalty will not be serious. There are some applications in which fouling is unlikely to be of concern, for example, gas-gas heat exchange in a closed Brayton cycle used for extracting power from a nuclear reactor, and for these applications the MTS heat exchanger may be appealing. For other applications, it may be possible to reduce fouling to acceptable levels by continuous cleaning of the gas streams. We are in the process of evaluating several cleaning methods, including filtration and electrostatic precipitation [15].

Flow Maldistribution

The very small scale of the component modules of the MTS heat exchanger requires careful design of manifolds and baffles if flow maldistribution is not to be a problem. Mueller and Chiou give a general review of this problem in [13]. Of the causes of flow maldistribution discussed in [13], poor manufacturing tolerances are not thought to be a problem for tube-side flow at the level of individual MTS modules: the method of manufacture gives a very uniform tube size. As the experimental results suggest, however, shell-side maldistribution does appear to be a serious problem in the prototype banks. We are currently investigating the extent and control of shell-side flow maldistribution, and the optimal design of manifolds and baffles.

Applications

Surface Cooling

There are applications where it is necessary to handle extremely high surface heat fluxes (the first-wall in a fusion